Kinetics or thermodynamics? Extolling their role to modulate the crystal phases and luminescence of $KY_3F_{10}:Eu^{3+}$ powders

Pablo Serna-Gallén* (pserna@uji.es), Héctor Beltrán-Mir, Eloísa Cordoncillo

Departamento de Química Inorgánica y Orgánica, Universitat Jaume I, Av. Sos Baynat s/n 12071, Castelló de la Plana, Spain

*Corresponding Author

Supporting Information

S1. Previous experiments and the scope of the present study

We recently published a paper in which a new coprecipitation method was developed to obtain nanospheres of the metastable δ-phase of KY_3F_{10} at room temperature (25 °C) [S1]. Since α-KY_3F_{10} is the thermodynamic phase, we thought that this new process could be a good candidate to explore the influence of kinetic and thermodynamic factors on the reaction system and the final product. In order to check whether it was possible to obtain single α-phase using the same experimental procedure and reagents concentration that had been employed to obtain the metastable δ-phase, several experiments were carried out in which the temperature of the reaction medium was set to 80 °C, which could, a priori, facilitate the formation of the most thermodynamic crystal structure.

However, as depicted in **Figure S1**, it was not possible to properly achieve only the thermodynamic phase (α). When the reaction was conducted at 80 °C for 1 hour, the presence of α-KY_3F_{10} was notable, but even at reaction times of 1 and 7 days, there were still considerable impurities of δ-KY_3F_{10}. Indeed, for high maturing times (7 days), the sample also started to decompose in YF_3. Very similar results (not shown because they do not add significant

information) were obtained at lower reaction temperatures but with the proviso that higher maturing times were necessary to achieve the higher concentration/decomposition of α-KY_3F_{10}.

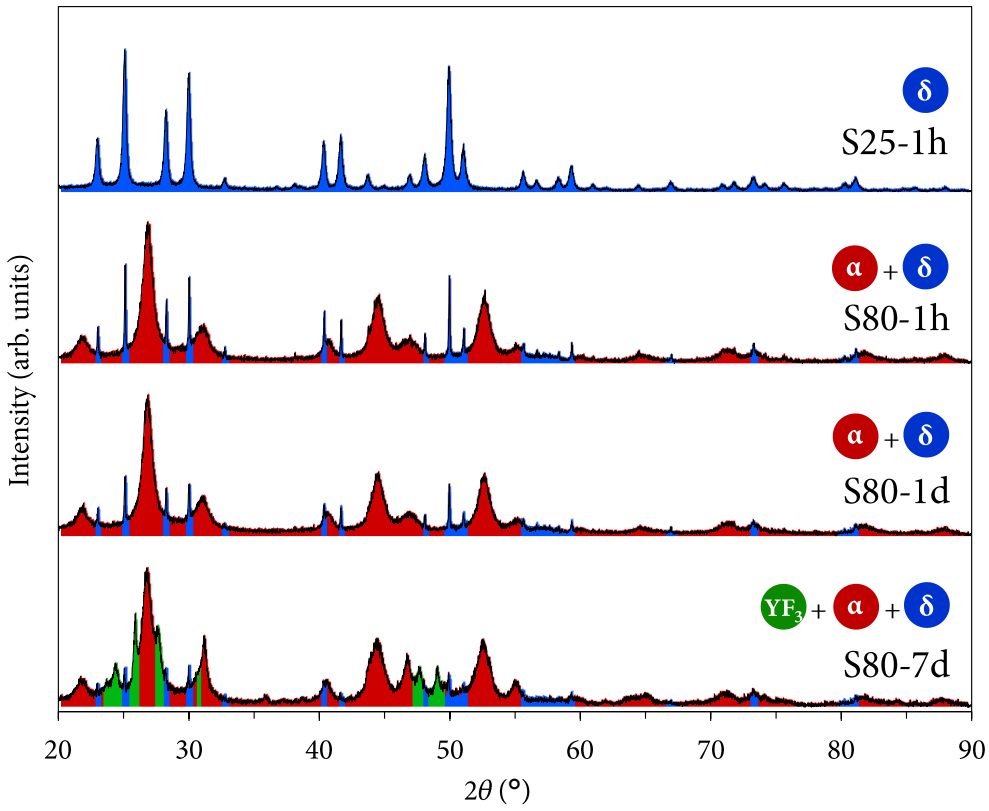

Figure S1. XRD patterns of the powders prepared under different reaction conditions of time and temperature. The area under the peaks corresponding to each crystal structure has been colored for clarity purposes: blue for δ-KY_3F_{10}, red for α-KY_3F_{10}, and green for YF_3. The XRD pattern corresponding to sample S25-1 h is the on published in Ref. [S1].

These results showed that such a methodology was not successful to isolate both compounds depending on the kinetic/thermodynamic factors. As the α-δ system is extremely delicate and sensitive to any change in the reaction medium, the new idea was to modify the concentration of the reagents so as to obtain, in a controlled manner (the fast addition procedure was discarded), a mixture of both phases at room temperature that could move the system toward the formation of one specific crystal phase depending on the kinetic and thermodynamic control. Therefore, in the present study, the reagents concentration was modified (the mmol and total amount of solvent

were the same, but the water volume of each solution was changed). **Table S1** underscores the concentrations used in the precedent [S1] and the present study.

Table 1. Reagents concentration (Ln = Y, Eu). The KF/HF solution was added dropwise to the Ln^{3+} solution.

Study	$[Ln^{3+}]$	[KF/HF]
Ref [S1]	0.15 (10 mL)	0.30 (10 mL)
This work	0.10 (15 mL)	0.60 (5 mL)

As outlined in the main text, this small change in the concentration of the reagents has a profound impact and allows us to properly proceed with the main scope of the study.

S2. Crystallographic characterization

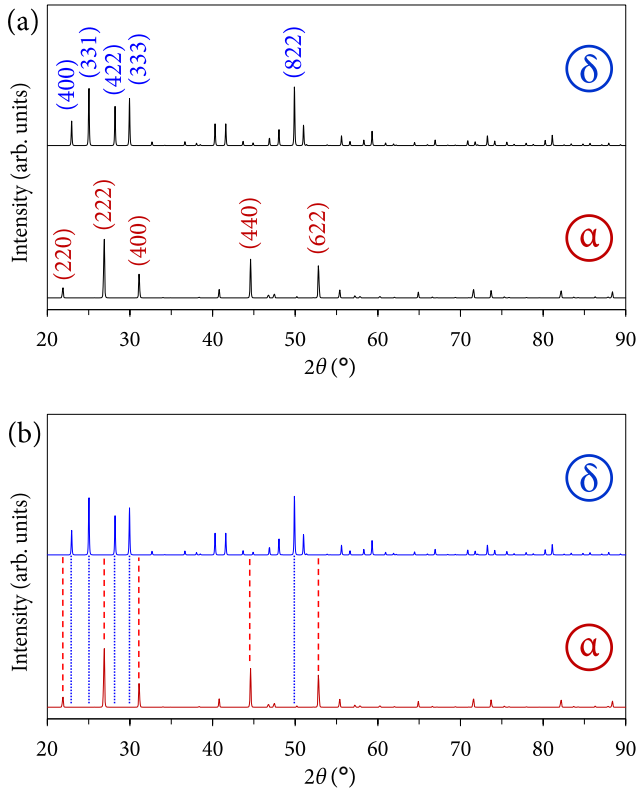

Figure S2. Pattern standards for δ-KY_3F_{10}·xH_2O (ICSD card 00-040-9643) and α-KY_3F_{10} (ICDD card 04-016-7073) highlighting (a) the Miller indices of the most useful diffraction peaks that can be used to identify the presence of these crystal structures, along with (b) guidelines to see at first glance that the diffraction peaks positions are different.

All the experimental diffraction patterns of the powders were refined using the Rietveld method by means of GSAS software. Pseudo-Voight functions were used to simulate the peaks shape and Chebyshev-1 functions with 10 coefficients were used to simulate the background.

Table S1. Refined unit cell parameter ($a = b = c$) for the different XRD patterns of the powders containing α-KY_3F_{10} and/or δ-KY_3F_{10}·xH_2O crystal phases.

T (°C)	α, a (Å)			δ, a (Å)		
	1 hour	1 day	7 days	1 hour	1 day	7 days
25	11.5240(17)	11.5341(15)	–	15.5097(19)	15.5028(13)	15.4994(9)
40	11.5374(21)	11.5312(15)	11.5392(19)	15.5034(26)	15.5098(14)	15.5087(16)
60	11.5365(15)	11.5483(24)	11.5385(8)	15.5043(21)	15.5060(30)	15.5079(12)
80	11.5482(18)	11.5450(16)	11.5488(15)	–	–	–

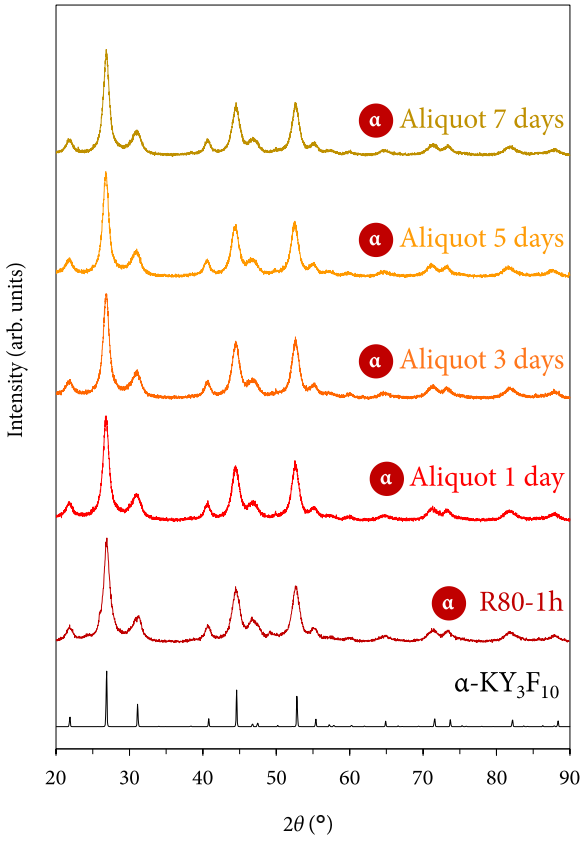

Figure S3. XRD patterns of the aliquots taken at different times from the reaction medium after synthesizing sample R80-1h and cooling it down to room temperature.

S3. Emission spectra recorded at different DTs

To accurately calculate the JO and *R* parameters, the emission spectra were recorded again setting a detector delay time (DT) of 10 ms, which ensures the avoidance of contribution from the higher excited state $^5D_1$. An example of the emission spectrum at different DTs is presented in **Figure S4** for sample R80-1h.

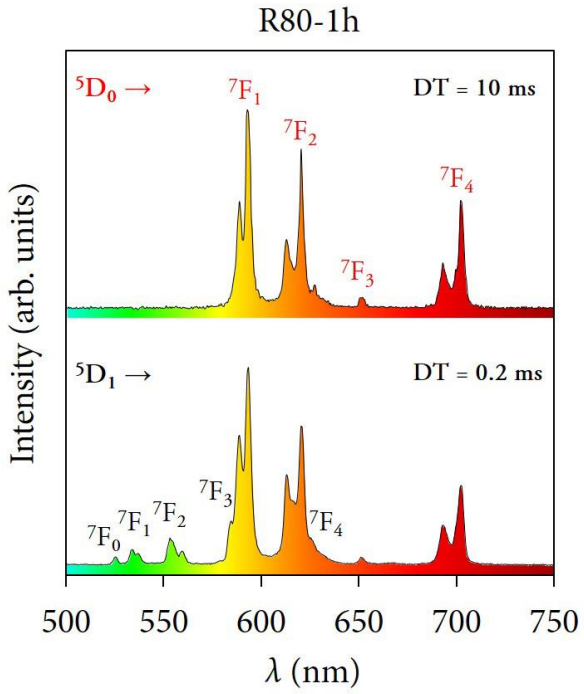

Figure S4. Room temperature emission spectra of sample R80-1h obtained with a delay time (DT) of 0.2 and 10 ms upon excitation at 395 nm highlighting the different $^5D_{0,1} \rightarrow {}^7F_J$ transitions.

S4. Lifetimes

Figure S5 depicts the results of fitting the experimental points of time-resolved luminescence for the $^5D_0$ state following different models for sample R25-1h as an example. As commented in the main text, the best choice is the double exponential model, since it provides the most accurate fit. The mathematical models used are the following:

(a) Double exponential model, **Figure S5(a)**, which corresponds to the formula:

$$I(t) = I_1 \exp\left(\frac{-t}{\tau_{\text{obs }1}}\right) + I_2 \exp\left(\frac{-t}{\tau_{\text{obs }2}}\right) \quad \text{(S1)}$$

(b) Single exponential model, **Figure S5(b)**, which corresponds to the formula:

$$I(t) = I_0 \exp\left(\frac{-t}{\tau_{\text{obs}}}\right) \quad \text{(S2)}$$

(c) Single logarithmic model, **Figure S5(c)**. It has also been contemplated because some readers might be more familiar with the semi-logarithmic plot of the luminescence intensity vs. time. Expression S2 is simplified into a linear equation from which the lifetime can be easily extracted from the slope of the line:

$$\ln I(t) = \ln I_0 - \frac{t}{\tau_{\text{obs}}} \quad \text{(S3)}$$

However, this mathematical approach, along with the corresponding plot, is of interest for cases when the decay curve exhibits a single exponential decay. Applying natural logarithmic to expression S2 would result in a complex formula that is not straightforward to simplify as in the latter case.

Figure S5 also shows some insights into the plot when it can be easily appreciated that when using the single models, the experimental points are partially deviated from the fitting curve, thus obtaining worse correlation coefficients of the fits (R^2).

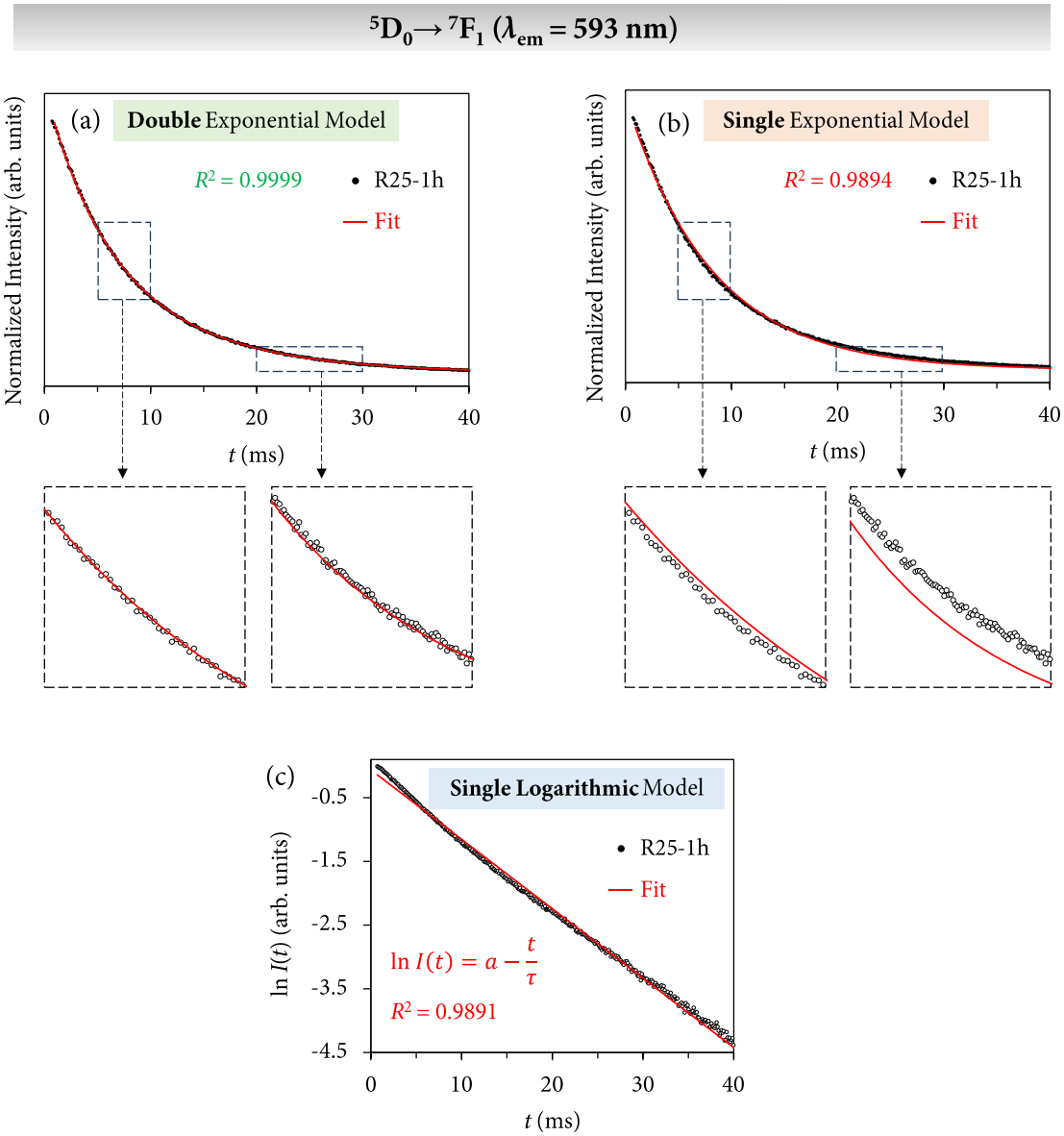

Figure S5. Normalized decay curves acquired at room temperature with a DT = 0.2 ms exciting the samples at 395 nm and collecting the emission at 593 nm ($^5D_0 \rightarrow {}^7F_1$ transition) for the lowest-lying excited state $^5D_0$. Different fitting models have been used: (a) double exponential, (b) single exponential, and (c) single logarithmic. For all the plots, the fitting curves are shown along with the corresponding correlation coefficients (R^2).

In a similar way, **Figure S6** depicts the results of fitting the experimental points of time-resolved luminescence for the $^5D_1$ state following the different models. It must be noted that now the discrepancy between double and single fitting is more accentuated.

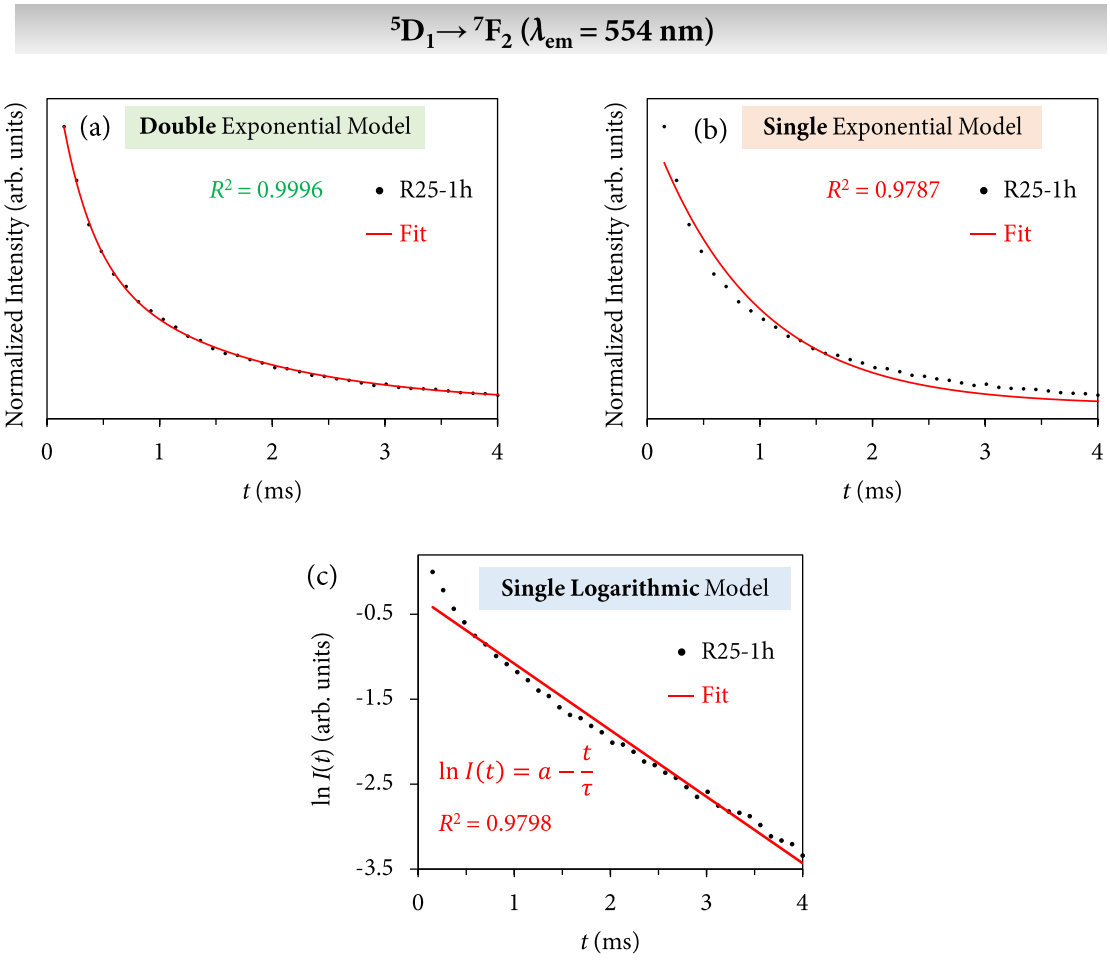

Figure S6. Normalized decay curves acquired at room temperature with a DT = 0.2 ms exciting the samples at 395 nm and collecting the emission at 554 nm ($^5D_1 \rightarrow {}^7F_2$ transition) for the higher excited state $^5D_1$. Different fitting models have been used: (a) double exponential, (b) single exponential, and (c) single logarithmic. For all the plots, the fitting curves are shown along with the corresponding correlation coefficients (R^2).

References

[S1] P. Serna-Gallén, H. Beltrán-Mir, E. Cordoncillo, R. Balda, J. Fernández, A site-selective fluorescence spectroscopy study of the crystal phases of KY_3F_{10}: Leveraging the optical response of Eu^{3+} ions, J. Alloys Compd. 953 (2023) 170020. https://doi.org/10.1016/j.jallcom.2023.170020.